Tumor and Stem Cell Biology

S100A4 Elevation Empowers Expression of Metastasis Effector Molecules in Human Breast Cancer

Thamir M. Ismail, Daimark Bennett, Angela M. Platt-Higgins, Morteta Al-Medhity, Roger Barraclough, and Philip S. Rudland

Abstract

Many human glandular cancers metastasize along nerve tracts, but the mechanisms involved are generally poorly understood. The calcium-binding protein S100A4 is expressed at elevated levels in human cancers where it has been linked to increased invasion and metastasis. Here we report genetic studies in a *Drosophila* model to define S100A4 effector functions that mediate metastatic dissemination of mutant Ras-induced tumors in the developing nervous system. In flies overexpressing mutant Ras^{Val12} and S100A4, there was a significant increase in activation of the stress kinase JNK and production of the matrix metalloproteinase MMP1. Genetic or chemical blockades of JNK and MMP1 suppressed metastatic dissemination associated with S100A4 elevation, defining required signaling pathway(s) for S100A4 in this setting. In clinical specimens of human breast cancer, elevated levels of the mammalian paralogs MMP2, MMP9, and MMP13 are associated with a 4- to 9-fold relative decrease in patient survival. In individual tumors, levels of MMP2 and MMP13 correlated more closely with levels of S100A4, whereas MMP9 levels correlated more closely with the S100 family member S100P. Overall, our results suggest the existence of evolutionarily conserved pathways used by S100A4 to promote metastatic dissemination, with potential prognostic and therapeutic implications for metastasis by cancers that preferentially exploit nerve tract migration routes. *Cancer Res; 1–12. ©2016 AACR.*

Introduction

Certain tumor cells have a propensity to invade the neighboring tissue and eventually establish new secondary tumors or metastases while others cannot (1, 2). These results suggest that a specific set of genes, different from those involved in the production of the neoplasia, are involved in promoting a complex series of steps to form metastases (3). The protein products of such genes have been termed metastasis-inducing proteins (MIP). One such gene/protein is *S100A4* (4), a member of the S100-calcium-binding protein family (5). Although *S100A4* cannot promote tumor formation directly, it can stimulate the remaining steps in the metastatic cascade in model rodent systems by combining with oncogenes such as Ras^{Val12} and *neu* (4, 6). Moreover, *S100A4* is overexpressed in human primary tumors and is associated with the premature death of patients with different types of metastatic carcinomas, including those from the breast (7), oral mucosa, bladder, pancreas, prostate, colorectum, esophagus, lung, stomach, and thyroid glands (8). The elevation of S100A4 can trigger multiple biological functions, including cell migration, invasion, extracellular matrix remodeling, and angiogenesis (8, 9). How-ever, it is unknown what are the biologically relevant molecular events from the plethora triggered by S100A4 in cultured mammalian cells (10). To generate a genetically tractable experimental model to investigate the molecular events triggered by S100A4, we have for the first time expressed human *S100A4* in the fruit fly, *Drosophila melanogaster* by targeting its expression to the developing eye lobes (11) and not elsewhere in the brain or CNS (12, 13). *Drosophila* has conserved signal transduction pathways for cell cycle, growth control, and cell-to-cell communication (14) and a larval phase of only a few days, which can be interrogated by inhibitory chemicals applied directly to the growth medium. In addition, 70% of human cancer genes are conserved in the *Drosophila* model, but importantly none of the S100 family proteins are present (15). Overexpression of oncogenic Ras (Ras^{Val12}) causes the formation of tumors in the epithelial tissues of *Drosophila* (16), and these can be transformed into a malignant phenotype by disruption of suppressor genes such as *scribble (scrib)* and *lethal2* (17). In this new model we have for the first time generated transgenic flies capable of conditionally-expressing the open-reading frame of human *S100A4* under *GAL4/UAS*-control (18). We show, after multiple crosses, that the *S100A4* gene is required to disseminate Ras^{Val12} tumor cells from the optic lobes to the ventral nerve cord (VNC) and further afield in fly larvae. The combination of Ras^{Val12} and loss of *scrib* in *Drosophila* activates the JNK pathway and this activation induces the matrix metalloproteinase MMP1 to allow dissemination of the cancer cells in the Ras oncogenic system (16). Therefore, we have assessed whether c-Jun and *Drosophila* MMP1 are downstream targets for promoting dissemination in our Ras^{Val12}/S100A4 novel larval model using fly genetics and inhibitory chemicals, and whether there is a uniquely similar association between S100A4 and mammalian MMPs in human breast cancer.

Department of Biochemistry, Institute of Integrative Biology, University of Liverpool, Liverpool, United Kingdom.

Corresponding Author: Philip S. Rudland, University of Liverpool, Crown Street, Liverpool, Merseyside L69 7ZB, United Kingdom. Phone: 4415-1795-4474; Fax: 4415-1795-4408; E-mail: rudland@liverpool.ac.uk

Materials and Methods

Expression of S100A4 in Drosophila melanogaster

Human S100A4 wild-type (S100A4wt; ref. 19) and inactive mutant S100A4Δ2 (20) were cloned and expressed in transgenic flies as described in Supplementary Methods. Stable transgenic lines were checked for S100A4 expression by crossing with da-GAL4 flies (18) and Western blotted. Resultant S100A4wt and S100A4Δ2 progeny produced (mean ± SE) similar 7.7 ± 0.6 ng and 8.8 ± 0.7 ng S100A4 protein per 20 flies, respectively, compared with undetectable levels (<0.1 ng) in parental controls [Student t test (STT); $P = 0.29$]. Remaining details are in Supplementary Methods. All initial Drosophila strains were described previously (21), remaining details are in Supplementary Methods. The flies were maintained in standard yeast agar medium at 25°C in a 12-hour light–dark incubator (21).

Metastatic assay

The eyeless-FLP–induced recombination of the FRT-flanked γ linker in Act>γ>GAL4 results in reconstitution of Actin-GAL4 and expression of UAS-GFP, and other UAS elements, in the developing eye (22). Dissemination of GFP from its original site of eye-antennal discs to VNCs was scored for each genotype/experimental condition on a scale of 0 to 3 (16). GFP localized in the optic lobes scored zero (stage 0), GFP on one side of the VNC scored 1 (stage I), on two sides of VNC scored 2 (stage II), and dissemination further into the VNC scored 3 (stage III). Average stage score of metastasis (ASSM) ±SE was recorded for each genotype/experimental condition. Fluorescent staining is described in Supplementary Methods. Confocal images of GFP were captured (21) and analyzed using ImageJ software (23), as described in Supplementary Methods. Corrected integrated fluorescence intensity (CIFI) = integrated intensity − (area of selected background brain × mean fluorescence density of background) (23). Mean CIFI ± SE was recorded.

Western blot analysis

This is described in Supplementary Methods. To correct for any loading differences, original intensity of each band was divided by that of actin. Intensity of each band for a particular larval group was then expressed as a ratio of that in the Ras^{Val12} larvae. Mean value of three experiments ±SE was recorded. To ensure the intensity of band signals lay within the linear range, a plot of band intensity against μg GAPDH was drawn ($y = 43947 \times -42398$, $r^2 = 0.997$) and band intensity for any protein outside the linear range was excluded from the data and if necessary the gel was rerun with higher or lower levels of total protein.

Drug treatment

Inhibitors, JNK-IN-8 (kindly provided by Nathanael S. Gray, Harvard Medical School, Boston, MA; ref. 24) and batimastat (cat. no.: SML0041; Sigma-Aldrich; ref. 25) were added directly from 1 mg/mL stock dissolved in DMSO to larval medium preheated to 55–60°C. Same concentration of DMSO was added to controls without inhibitors. The drugs were incubated with the larvae continuously until harvesting at the third instar stage, equivalent to 7 days.

Statistical analyses

The significance of the difference between two categorical groups for each genotype, those with and those without
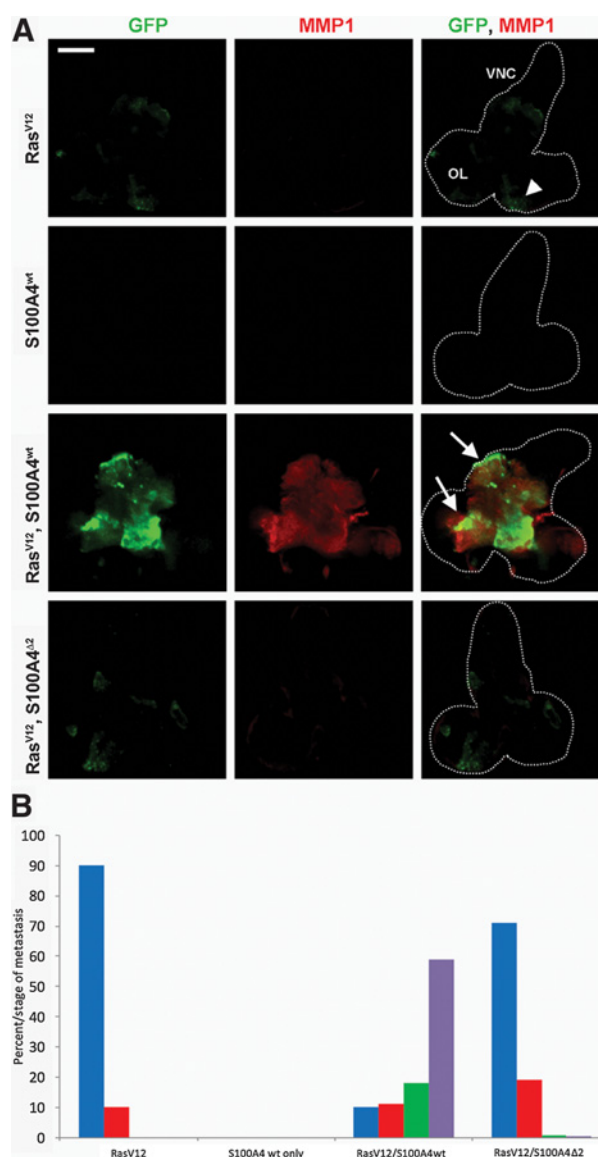
Figure 1.
A, Fluorescent images of GFP and MMP1 in larval CNS of different male recombinant Drosophila. CNS was dissected from third instar larvae of Drosophila with the following backgrounds: Ras^{Val12}(RasV12) only; S100A4 wild type (S100A4wt) only; Ras^{Val12}, S100A4 wild type (RasV12/S100A4wt); and Ras^{Val12}, S100A4Δ2 (RasV12/S100A4Δ2). Representative CNS images show green fluorescence due to endogenous GFP, red fluorescence due to fluorescently labeled antibodies to matrix metalloproteinase1(MMP1), and merged fluorescent images are due to GFP and anti-MMP1. The outline of the relevant structures of the brain including optic lobes (OL) and ventral nerve cord (VNC) are indicated by the broken white line. The region which clearly expresses MMP in Ras^{Val12}, S100A4 transgenics (arrows), and the same region in Ras^{Val12} transgenics (arrow head) are shown (Scale bar, 100 μm). **B,** Histogram of resultant recombinant larvae. The percentage (percent) larvae with different stages (0–III) of metastasis from the optic lobes to the ventral nerve cords (VNC) is shown for the recombinant Drosophila. The VNC of at least 50, third instar larvae were scored for the extent of metastasis on a sliding scale (Materials and Methods): from stage 0 (blue), stage I (red), stage II (green), and stage III (purple). Larvae containing Ras^{Val12}/S100A4 were significantly different from these containing Ras^{Val12} alone, S100A4 alone, and Ras^{Val12}/S100A4Δ2 (Fisher exact test $P < 0.0001$) and between larvae containing Ras^{Val12} and Ras^{Val12}/S100A4Δ2 ($P = 0.012$).

Q5
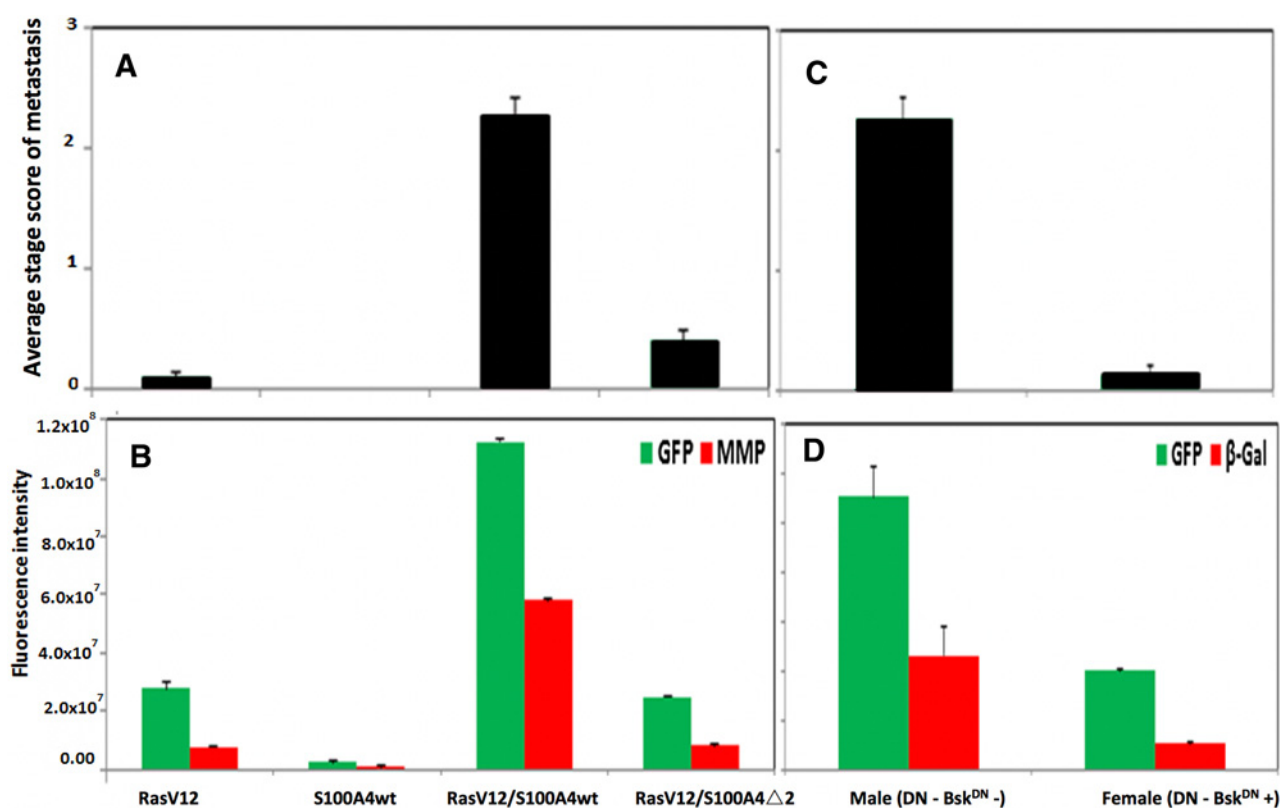
Figure 2.
Tumor dissemination in different recombinant *Drosophila* larvae. **A,** Average stage of metastatic spread in *Ras*^{Val12}/*S100A4* flies. ASSM of the primary tumor in the optic lobe spreading to the VNC is shown for male recombinant *Drosophila* with genetic backgrounds of: *Ras*^{Val12} (RasV12), *S100A4 wild type only* (S100A4wt), *Ras*^{Val12} plus S100A4 wild type (RasV12/S100A4wt), and *Ras*^{Val12} plus *S100A4mutantΔ2* (RasV12/S100A4Δ2). At least 50 larvae were scored (Materials and Methods) and results are expressed as mean ± SE. Both double transgenic flies were significantly different from flies with *Ras*^{Val12} genotype (STT.$P \leq 0.005$) and *Ras*^{Val12}/*S100A4wt* from *Ras*^{Val12}/*S100A4Δ2* genotype ($P = 0.0001$). **B,** Fluorescence intensity of CNS images of *Ras*^{Val12}/*S100A4* flies. Endogenous fluorescence from GFP (green) and from exogenously-added labeled antibody to MMP1 (red) were recorded. CIFI of images of the dissected CNS from the same larvae in A were computed as described in "Methods." Mean ± SE is shown. For GFP green fluorescence, *Ras*^{Val12}/*S100A4wt* versus *Ras*^{Val12} only, *S100A4wt* only, or *Ras*^{Val12}/*S100A4Δ2* (STT.$P < 0.0001$); *Ras*^{Val12} vs. *Ras*^{Val12}/*S100A4Δ2* ($P = 0.49$). For MMP-1 red fluorescence, *Ras*^{Val12}/*S100A4wt* versus *Ras*^{Val12} only, *S100A4wt* only, and *Ras*^{Val12}/*S100A4Δ2* (STT.$P < 0.0001$); but *Ras*^{Val12} versus *Ras*^{Val12}/*S100A4Δ2* larval CNS ($P = 0.15$). **C,** Average stage of metastatic spread in male and female JNK-suppressed *Ras*^{Val12}/*S100A4* flies. ASSM of the primary tumor in the optic lobe spreading to the VNC is shown for recombinant *Drosophila* male and female larvae with the genetic backgrounds of *Ras*^{Val12}/*S100A4wt* in which the *Bsk*^{DN} dominant suppressor of JNK is expressed only in female flies. At least 20 larvae were scored as in **A**. Results are expressed as mean ± SE and there was a highly significant difference (STT.$P < 0.0001$). **D,** Quantification of the levels of fluorescent GFP and β-galactosidase in JNK suppressed flies. Endogenous fluorescence from GFP (green) and from exogenously-added labeled antibody to β-galactosidase (β-Gal) (red) were recorded. CIFI of images of the dissected CNS from the same larvae as in C were computed for male and female *Drosophila* with the *Ras*^{Val12}/*S100A4wt* genetic background. Mean ± SE is shown. The β-galactosidase is a marker of the activity of JNK (Materials and Methods). For GFP green fluorescence and β-galactosidase red fluorescence, significant reduction for female versus male *Ras*^{Val12}/*S100A4wt* larvae (STT.$P < 0.0001$ and $P = 0.004$, respectively).

metastases was determined by Fisher exact test, recording two-sided values of *P*. The significance of the difference in ASSM, in CIFI for GFP and MMP1, and in mean corrected intensity of each protein band in Western blots were calculated using two-sided Student *t* test (Stats Direct). Differences considered significant when $P < 0.05$.

Patients and specimens

A retrospective study was undertaken using samples of 183 primary tumors from unselected breast cancer patients, as described previously (26, 27). Ethical approval was obtained from NRES Committee, North West REC.Ref. 12/NW/0778, Protocol no. UoL000889, IRAS no. 107845. Samples were preserved in neutral buffered-formalin and embedded in paraffin-wax, as described previously (7).

IHC staining

This is described in Supplementary Methods. Western blots of breast cell lines verified the specificity of all three mAbs to MMPs yielding apparent molecular weights of 73,99,75 kDa for secreted latent MMP2, 9, 13, respectively, consistent with those reported recently (28). Remainders were verified previously (27). IHC-stained sections were analyzed and scored (7, 26, 28, 29), as recorded in Supplementary Methods. Association of staining for MMP2, 9, and 13 with patient survival time is reported in Supplementary Methods.

174 ## Results

175 ### Cooperation of Ras^{Val12} and S100A4 in producing metastases in
176 recombinant *Drosophila*

177 The brain containing the CNS was dissected from at least fifty,
178 third instar larvae of different recombinant *Drosophila*. Male larvae
179 with the genetic background Ras^{Val12} alone (Ras^{Val12} larvae)
180 produced GFP-fluorescent tumors almost exclusively in the eye
181 lobes (Fig. 1A) of 48 of 53 cases, with only 5 of 53 cases extending
182 into one or the other side of the VNC (Fig. 1B). Extent of metastasis
183 was semiquantified as described in Materials and Methods to
184 produce an ASSM. There were no GFP-tumor deposits in the eye
185 lobes or elsewhere in S100A4 larvae (Figs. 1A and B and 2A). The
186 Ras^{Val12}/S100A4wt recombinant larvae produced metastasis to the
187 VNC (Fig. 1C) in a significantly higher number of 53 of 59 cases
188 [Fisher exact test, P (FET.P) < 0.0001; Fig. 1B], increasing the ASSM
189 by a significant 24-fold over Ras^{Val12} larvae [Student *t* test P (STT.P)
190 < 0.0001; Fig. 2A]. There was also extensive metastasis to other
191 organs, particularly to the gut and gonads (Supplementary Fig.
192 S1). The Ras^{Val12}/S100A4Δ2 inactive mutant larvae (Materials and
193 Methods) produced a significantly lower number of 16 of 56 with
194 metastasis to the VNC (FET.P < 0.0001; Fig. 1B), with significant
195 5.7-fold reduction in ASSM compared to Ras^{Val12} larvae (STT.P =
196 0.0001; Figs. 1A and 2A). The CIFI of GFP (Materials and Meth-
197 ods) for images taken of the dissected CNS of Ras^{Val12} larvae
198 was increased by a significant 4.1-fold in Ras^{Val12}/S100A4wt
199 larvae (STT.P < 0.0001; Fig. 2B), but there was no significant
200 difference in CIFI of Ras^{Val12}/S100A4Δ2 mutant larvae compared
201 with Ras^{Val12} larvae (STT.P = 0.49; Fig. 2B).

202 ### Quantification of Ras, GFP, and S100A4 levels by Western blot
203 analysis

204 Antibodies to S100A4 detected a specific band of the correct
205 apparent molecular weight of 9 kDa in all fly lines containing the
206 S100A4wt or S100A4Δ2 mutant gene, but no corresponding band
207 in larvae containing Ras^{Val12} alone (Supplementary Fig. S2).
208 Larvae containing the Ras^{Val12}/S100A4wt and Ras^{Val12}/S100A4Δ2
209 genes produced a significant increase in Ras and a similar increase
210 in GFP over that in larvae containing Ras^{Val12} alone (STT.P <
211 0.001; Table 1). Protein bands of Ras and GFP were observed at
212 the correct molecular weights (21 and 27 kDa, respectively;
213 Supplementary Fig. S2 and Table 1). There was also highly

215 significant increases of 220 ± 5- and 85 ± 11-fold in S100A4
216 protein in larvae containing the Ras^{Val12}/S100A4wt and Ras^{Val12}/
217 S100A4Δ2 genes, respectively (P < 0.0001; Table 1), when nor-
218 malized to GFP. Thus, there is a significant association of expres-
219 sion of active S100A4 and metastasis in this model system.

220 ### Increased levels of activated JNK and MMP1 in Ras and
221 S100A4-overexpressing larvae

222 Levels of JNK in Ras^{Val12} and Ras^{Val12}/S100A4wt larvae were not
223 significantly different in Western blots analysis (STT.P =
224 0.50; Table 1). However, levels of activated phospho-JNK and
225 MMP1 at the reported molecular weights of 46 and 52 kDa,
226 respectively (30), rose significantly by 13.1 ± 0.6- and 3.8 ±
227 0.1-fold, respectively, when normalized to GFP, in Ras^{Val12}/
228 S100A4wt compared to Ras^{Val12} larvae (P < 0.0001; Supplementary
229 Fig. S2 and Table 1). There was no significant increase in phospho-
230 JNK, JNK, and MMP1 in Ras^{Val12}/S100A4Δ2 compared to Ras^{Val12}
231 larvae. In S100A4wt larvae alone, the levels of phospho-JNK, JNK,
232 and MMP1 were significantly lower (P < 0.0001, P < 0.0001, P =
233 0.02; Supplementary Fig. S2 and Table 1), probably reflecting the
234 absence of any primary tumor (Figs. 1A and B and 2A). There was
235 also a modicum of red fluorescence for MMP1 in the eye lobes of
236 Ras^{Val12} larvae (Fig. 1A and B), which rose significantly in Ras^{Val12}/
237 S100A4wt larvae (P < 0.0001; Fig. 2B) showing extensive staining
238 of the VNC (Fig. 1A and B). There was no significant difference in
239 CIFI for Ras^{Val12} and Ras^{Val12}/S100A4Δ2 larvae (Fig. 2B).

240 ### Activated JNK and MMP are downstream effectors in Ras and
241 S100A4-overexpressing larvae

242 To determine the requirement for JNK signaling in the meta-
243 static phenotypes, we expressed dominant-negative JNK encoded
244 by *basket* (Bsk^{DN}), together with Ras^{Val12} and S100A4. When
245 female and male siblings with and without Bsk^{DN}, respectively
246 (Materials and Methods) were examined, 15/15 male, but only 2/
247 15 female larvae produced extensive metastases to the VNC (FET.P
248 < 0.0001; Supplementary Fig. S3). ASSM and CIFI were reduced by
249 a significant 17- and 2.8-fold in female larvae, respectively (STT.P
250 < 0.0001; Fig. 2C and D). The expression of a genetically-engi-
251 neered marker of JNK activity, *puc-LacZ* was followed by its
252 induction of β-galactosidase (Materials and Methods; Supple-
253 mentary Fig. S3). The CIFI for red fluorescent antibody to β-galac-
254 tosidase fell significantly by 4.7-fold in females (P = 0.004;

Q6 **Table 1.** Quantification of Western blots of different *Drosophila* lines

Antibody to[a]	Mean relative abundance[b]			
	Ras^{Val12}	S100A4wt	Ras^{Val12}/S100A4wt	Ras^{Val12}/S100A4Δ2
(A) Ras	1 ± 0.05	0.0097 ± 0.001	3.56 ± 0.08[c]	1.96 ± 0.16[c]
(B) GFP	1 ± 0.04	0.011 ± 0.002	3.50 ± 0.05[c]	1.60 ± 0.10[c]
(C) S100A4	1 ± 0.06	9.62 ± 2.1	742 ± 19[d]	136 ± 18[d]
(D) P-JNK	1 ± 0.01	0.19 ± 0.02[e]	40.5 ± 0.2[d]	1.32 ± 0.08
(E) Total JNK	1 ± 0.04	0.23 ± 0.01[e]	1.15 ± 0.07	1.04 ± 0.10
(F) MMP	1 ± 0.04	0.40 ± 0.07[f]	13.1 ± 0.3	0.498 ± 0.001
MMP	1 ± 0.04	nd	2.17 ± 0.08[g]	nd

Abbreviation: nd, not determined.
[a]Ten μg protein larval extracts were treated with the antibody shown in Western blots of Supplementary Fig. S2.
[b]Mean relative abundance after scanning the blots by densitometry (Materials and Methods) and the area under the peak corresponding to each protein was first normalized to that of actin and then ratioed to the level of that protein in the Ras^{Val12} male larvae which was arbitrarily set at 1. Mean relative abundance ± SE from three separate experiments.
[c]Student *t* test P < 0.001 over Ras^{Val12} male larvae.
[d]Student *t* test P < 0.0001 over Ras^{Val12} male larvae or S100A4wt male larvae.
[e]Student *t* test P < 0.0001 over Ras^{Val12} male larvae.
[f]Student *t* test P = 0.02 over Ras^{Val12} male larvae.
[g]Student *t* test P < 0.0001, for female over male larvae.

257 Supplementary Fig. S3 and Fig. 2D). In Western blots analysis, the
258 level of MMP1 protein normalized to that in male Ras^{Val12} larvae
259 fell 6.0-fold from 13.1 ± 0.3 to 2.17 ± 0.08 in male versus female
260 larvae ($P < 0.0001$; Table 1).
261 When increasing concentrations of the JNK-IN-8 inhibitor (24)
262 were added to male $Ras^{Val12}/S100A4wt$ larvae, there was a signif-
263 icant fall in ASSM of 2.5-fold for 1 µmol/L (STT.$P < 0.0001$), but
264 thereafter a more gradual stepwise decline; the overall fall being
265 5.8-fold ($P < 0.0001$; Supplementary Fig. S4A and S4B; Fig. 3A).
266 There was a similar significant decline in CIFI for GFP of 2.7-fold
267 ($P = 0.002$) for 1 µmol/L inhibitor and then successive significant
268 decreases; the overall fall being 11.4-fold ($P < 0.0001$) (Fig. 3A).
269 There was also a similar significant decline in CIFI for antibodies
270 to endogenous MMP1 upon addition of 1 µmol/L JNK-IN-8
271 (Supplementary Fig. S4A and S4B; $P = 0.0005$), then further
272 successive significant decreases; the overall fall being 8.3-fold
273 Q7 ($P < 0.0001$; Fig. 3A).
274 When increasing concentrations of the inhibitor of MMP activ-
275 ity, Batimastat (25) was added to $Ras^{Val12}/S100A4wt$ larvae, there
276 were significant falls in ASSM of 3.4-fold for 5 µmol/L ($P <$
277 0.0001), but thereafter the decline was more gradual; the overall
278 fall being 16.4-fold ($P < 0.0001$; Supplementary Fig. S4C and
279 S4D; Fig. 3B). There was a similar significant decline in CIFI for
280 GFP of 3.5-fold ($P = 0.0002$) for 5 µmol/L inhibitor and then
281 successive nonsignificant decreases. The overall fall was 8.4-fold
282 ($P < 0.0001$; Fig. 3B). There was also a rapid significant decline
283 in CIFI for antibodies to endogenous MMP1 upon addition of
284 5 µmol/L batimastat (Supplementary Fig. S4C and S4D) of 5.2-
285 fold ($P = 0.028$), then nonsignificant successive falls; the overall
286 fall being 10.3-fold ($P < 0.0001$; Fig. 3B). Thus, a definite pathway
287 has been established between S100A4 and MMP1 for induction of
288 metastasis in this model system.

289 **Association of MMPs with patient survival time in human breast**
290 **cancer**
291 Next, we investigated the relationship in human breast cancer
292 between the more commonly-occurring, mammalian MMPs,
293 MMP2, 9, 13, and patient demise as a result of metastatic cancer
294 (31). On examination of 183 breast carcinomas for IHC for these
295 three MMPs, 32% to 67% contained carcinoma cells which were
296 negatively stained (<1% carcinoma cells stained), 19% to 26%
297 were borderline stained (1–5% carcinoma cells stained), and the
298 rest (15–47%) were stained to varying degrees (Fig. 4 and Sup-
299 plementary Fig. S5; Supplementary Table S1). There were also
300 some reactive stromal cells, mainly myofibroblasts, macrophages,
301 and neutrophils which stained (Fig. 4). Assessment of staining
302 class was made only for the malignant cells. Staining for individ-
303 ual MMPs was abolished by prior incubation of each antibody
304 with the requisite MMP (Supplementary Fig. S5).
305 To determine whether there was any association between
306 staining for the separate MMPs and of survival of patients,
307 Kaplan–Meier survival curves were plotted for different staining
308 groups. Overall, there was a significant difference in staining for
309 each MMP (Wilcoxon Gehan Statistics, $P < 0.001$). However, the
310 largest significant differences occurred between the ($\pm$) and (+)
311 staining groups for MMP2, 9, and 13, respectively (Supplemen-
312 tary Table S2). The 183 patients were therefore separated into two
313 categorical groups using a cutoff of 5% stained carcinoma cells for
314 each MMP. Only $11 \pm 4\%$ survived with positively stained
315 tumors, compared to $81 \pm 4\%$ with negatively stained tumors
316 for MMP2; $10 \pm 6\%$ vs. $58 \pm 4\%$ for MMP9; and $22 \pm 5\%$ versus
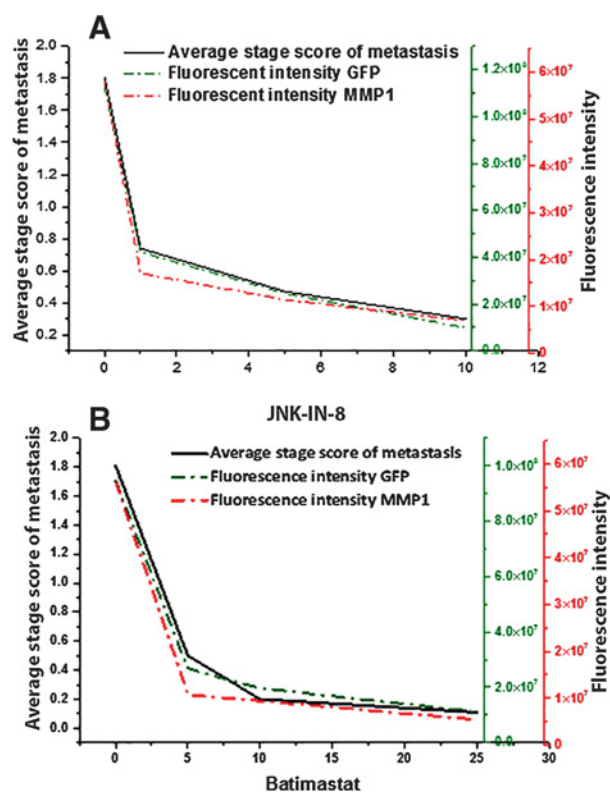
Figure 3.
Tumor dissemination in recombinant flies treated with either JNK-IN-8 (**A**) or Batimastat (**B**). *Drosophila* larvae with genetic background of $Ras^{Val12}/S100A4wt$ were fed either (**A**) 0, 1, 5, or 10 µmol/L of the JNK inhibitor JNK-IN-8 or (**B**) 0, 5, 10, or 25 µmol/L of the MMP1 inhibitor Batimastat in their medium (Materials and Methods). At least 20 larvae were scored and ASSM was computed as described in Materials and Methods. These same larvae were dissected, stained, and scored for endogenous green fluorescence from GFP and for red fluorescence from exogenously–added labeled antibody to MMP1. The CIFI was computed as described in Materials and Methods. Results are shown as mean $\pm$ SE. For ASSM, transgenic larvae fed 0 µmol/L of inhibitor were significantly higher than for larvae fed 1, 5, and 10 µmol/L JNK-IN-8 or for larvae fed 5, 10, and 25 µmol/L batimastat (STT.$P \leq 0.0001$). For JNK inhibitor-treated larvae, decrease in CIFI for those fed 1, 5, and 10 µmol/L JNK-IN-8 of 2.7, 4.6, and 11.4 folds, respectively for GFP fluorescence (STT.$P \leq 0.002$) and of 3.4, 5.1, and 8.3 folds, respectively, for MMP1-related fluorescence (STT.$P \leq 0.0005$). For MMP1 inhibitor-treated larvae, decrease in CIFI for those fed on 5, 10, and 25 µmol/L batimastat of 3.5, 4.8, and 8.4 folds, respectively, for GFP fluorescence (STT.$P \leq 0.0002$), and of 5.2, 5.9, and 10.3 folds, respectively, for MMP1-related fluorescence (STT.$P = 0.02$, 0.07, and 0.06, respectively).

75 $\pm$ 5% for MMP13 (Fig. 5). All differences were highly signif- 318
icant ($P < 0.001$) with median duration of survival of 47, 32, and 319
52 months for MMP2, 9, and 13 positively stained tumors versus 320
228 months in all cases of negatively stained tumors. These 321
corresponded to relative risks (RR) of death of 9.04 (95% CI, 322
5.32–15.36), 4.69 (95% CI, 2.89–7.62), and 4.87 (95% CI, 2.98– 323
7.97), respectively. Results for S100A4 with a cutoff of 5% were 324
similar to that for individual MMPs with only $9 \pm 4\%$ surviving 325
versus $80 \pm 4\%$ for unstained tumors, median survival time of 46 326
months versus 228 months ($\chi^2 = 71.8$, $P < 0.001$), and RR of 327
patient death of 9.96 (95% CI, 5.87–16.9; Supplementary Table 328
S3). Patients with tumors stained positively for all three MMPs 329
showed no significant increase in mortality (7% $\pm$ 6%), decrease 330
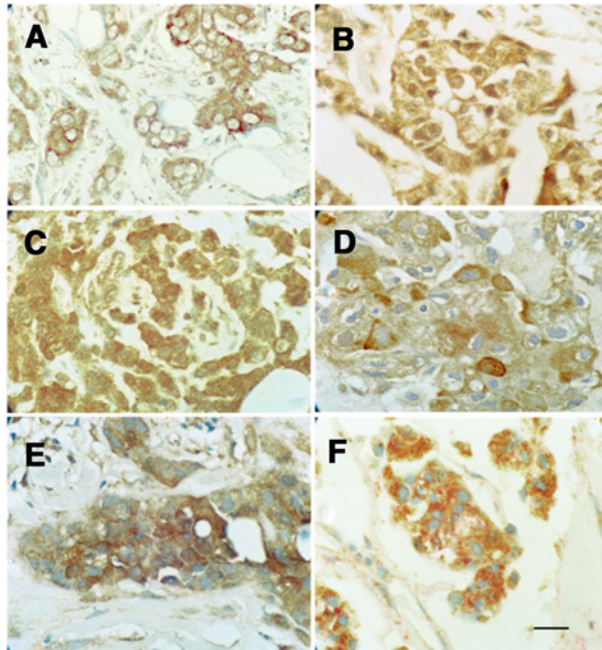
Figure 4.
Immunohistochemical staining of different breast carcinomas with antibody to MMP2 (**A**), MMP9 (**B**), or MMP13 (**C**) showing strong brown staining of the carcinoma cells' cytoplasm. Incubation with antibody to S100A4 (**D**) or S100P (**E**) showing strong, bead-like, cytoplasmic staining. **F,** Incubation with antibody to MMP2 with brown chromophore and to S100A4 with red chromophore showing most carcinoma cells were stained by both antibodies. Tumors were selected to show strong staining in **A** to **C** for their respective MMP, but the same tumor was stained in **D** to **F** as in **A** (×180; scale bar, 20 μm).

in median survival time (30 months), or increase in RR (4.96; 95% CI, 2.99–8.24) than staining for either MMP2 or MMP9 separately (Supplementary Table S2). When all three MMPs were included in Cox's multivariate regression analysis (Materials and Methods), the individual contributions made to the time of patient demise showed that staining for MMP2 ($P < 0.001$) and that for MMP9 ($P = 0.025$) were independently significant while that for MMP13 was not (Supplementary Table S3).

Association of MMPs with S100A4 and patient survival

Results for IHC staining for the 3 MMPs using a 5% cutoff were cross-tabulated against pathologic variables and IHC staining for S100A4, S100P (29), estrogen receptor α (ERα), progesterone receptor (PgR), c-erbB-2 (Her2), cytokeratin 5/6 (CK5/6), and CK14 (32). All these variables have been reported to influence survival times in the same set of patients (26). Positive staining for each of MMP2, 9, and 13 was associated strongly with positive staining for S100A4 when using a 5% cutoff for S100A4. This association was slightly reduced with staining for S100P using a 5% cutoff (Table 2). Significance of association was much more marked for staining for S100A4 than for S100P when using a 1% cutoff. There was also a significant association with staining for CK5/6 and usually for CK14 (Table 2). Positive staining for any MMP was not significantly associated with involved lymph nodes, high tumor grade, large tumor size, nor with positive staining for ERα, PgR, or c-erbB-2 (Table 2). There was also a highly significant association of staining for each pair of MMPs (Table 2 and Supplementary Table S4).

When staining for S100A4 was tested for its relative probability of association (RA) with that for the three MMPs using binary logistic regression, that with MMP2 was strongest at 4.21 ($P < 0.001$), that with MMP9 of 2.41 was not significant, and that with MMP13 of 2.17 ($P = 0.051$) was very nearly significant. When staining for each of the MMPs, in turn, was assessed with staining for S100A4, CK14, ERα, PgR, and c-erb-2, only that for S100A4 and partially that for CK14 proved to be significant (Supplementary Table S5). When repeated using a different cutoff for S100A4 (1% instead of 5%; Table 2) and additionally including that for S100P, staining for MMP2 was most closely associated with that for S100A4 (Supplementary Table S5). To determine whether the three MMPs were independent of S100A4 when related to patient survival, they were included in a series of Cox's multivariate regression analyses (Materials and Methods; Supplementary Table S3). When a single MMP and S100A4 were only included, staining for S100A4 always emerged as the most significant association with patient survival time. Similar results were obtained if staining for S100A4 and all three MMPs were included in the same analysis, S100A4 emerged as the most significant association followed by MMP2 and then MMP9, whereas that due to MMP13 was not significant (Supplementary Table S3).

To determine whether there was coexpression of the MMPs and S100 proteins, two breast carcinomas were chosen that were either moderately or strongly stained for MMP2, and these were IHC restained for S100A4/P, 3 MMPs, CK5/6, and CK14. Exactly the same areas were examined for each antigen. The percentage of stained cells for S100A4 was not significantly different from that for MMP2 and MMP13, while staining for S100P was not significantly different from that for MMP9 (Supplementary Fig. S6; and Supplementary Table S6). Staining for S100A4 or MMP2 was also not significantly different from that for CK5/6, but only in the MMP2 moderately-stained carcinomas; all the other paired combinations were significantly different (Supplementary Fig. S6; and Supplementary Table S6). When serial sections from three breast carcinomas strongly-staining for MMP2 were doubly IHC-stained for S100A4 with red and for MMP2 with brown chromophores on the same section, there were (mean ± SE) 80.2 ± 2.2% doubly stained cells, 6.9% ± 0.9% cells stained red for S100A4, 2.9% ± 0.4% cells stained brown for MMP2 and 9.1% ± 1.5% unstained cells (ANOVA, $F = 669.3$, 3 df, $P < 0.001$; Supplementary Fig. S7). Thus, S100A4 is associated with and partially confounded for patient survival by the three MMPs to varying degrees.

Discussion

We have shown for the first time that S100A4 can induce metastasis in the *Drosophila* model and that the oncogene Ras^{Val12} largely fails in this respect. The increase in number of larvae bearing VNC metastases (10-fold), in ASSM (24-fold), and in CIFI (4.1-fold) for $Ras^{Val12}/S100A4$ over Ras^{Val12} larvae demonstrates clearly that S100A4 promotes extensive dissemination to the VNC, as well as elsewhere in the larvae (Supplementary Fig. S1). The reason for the differences in fold increases is due to the method of measurement, the CIFI included GFP fluorescence due to the primary as well as the metastases, whereas the first two parameters relate only to the metastases. That larvae containing Ras^{Val12} and inactive $S100A4Δ2$ genes (20) show significantly less metastases (Fig. 1A, 2A, and B), demonstrates that the migratory/invasive ability of S100A4 (20) is required for its metastatic ability. That $S100A4$ larvae produce no tumors at all

Figure 5.
Association of immunohistochemical staining for MMPs with overall time of patient survival. Cumulative proportion of surviving patients as a fraction of the total for each year after presentation for patients with carcinomas classified as negatively-stained (set a solid line) or positively-stained (set b, dotted line) is shown for MMP2 (**A**), MMP9 (**B**), and MMP13 (**C**). Numbers of patients entering each year are shown below. The two curves are highly significantly different in each case (Wilcoxon statistic $\chi^2 = 71.81$, 32.50, or 41.90 for **A**, **B**, or **C**, respectively, 1 df, $P < 0.001$). Further details are shown in Supplementary Materials.
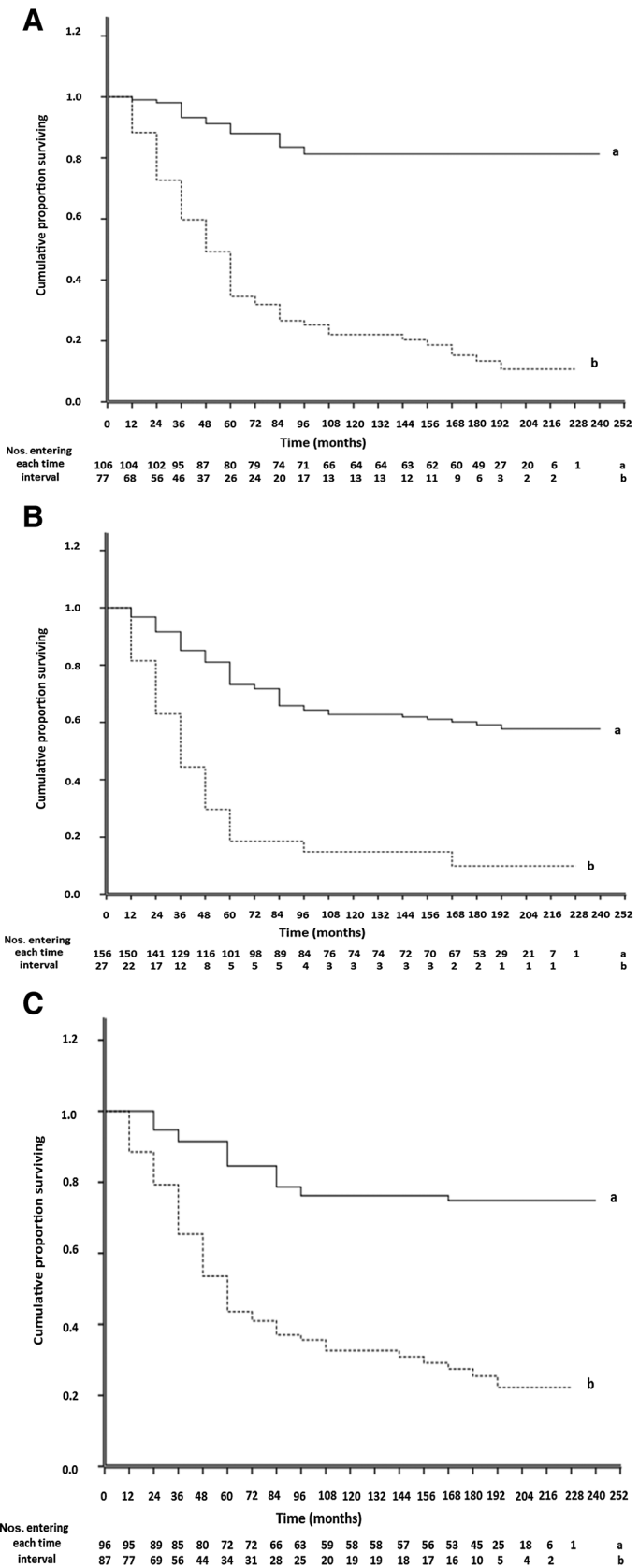
Table 2. Association of IHC staining for MMPs with other tumor variables

Tumor variable[a]	Patient[b] no.	Statistical significance[c]		
		MMP2	MMP9	MMP13
Lymph nodes	139	0.271	0.564	0.681
Grade	164	0.997	0.656	0.156
Tumor size	177	0.467	0.937	0.985
MMP2	183	—	9.0×10^{-7}	1.7×10^{-12}
MMP9	183	9.0×10^{-7}	—	1.2×10^{-7}
MMP13	183	1.7×10^{-12}	1.2×10^{-7}	—
S100A4 (5%)	183	6.6×10^{-9}	2.9×10^{-4}	2.4×10^{-6}
S100A4 (1%)	183	0^d	1.2×10^{-7}	1.9×10^{-8}
S100P (5%)	163	2.3×10^{-7}	2.2×10^{-3}	1.3×10^{-7}
S100P (1%)	163	1.6×10^{-4}	0.012	2.4×10^{-5}
CK14	172	5.7×10^{-7}	2.8×10^{-3}	0.372
CK5/6	173	1.6×10^{-6}	0.035	5.6×10^{-3}
ERα	181	1.00	1.0	1.0
PgR	172	0.995	0.983	0.549
C-erbB-2	183	0.660	1.00	0.809

[a]Lymph nodes with or without tumor deposits; grade, histologic grades I and II vs. grade III; tumor size <5 cm vs. >5 cm in diameter; presence or absence of IHC staining for molecular variables using 5% cutoff for MMP2, MMP9, MMP13, S100A4 (5%), S100P (5%), ERα, PgR, c-erbB-2, and using a 1% cutoff for S100A4 (1%), S100P (1%), CK14, and CK5/6.
[b]Number of patients from original 183.
[c]Probability P from Fisher exact test using the Holm–Bonferroni correction calculated as $1 - (1 - P)^n$, where $n = 12$ (Materials and Methods).
[d]Uncorrected $P = 7.7 \times 10^{-18}$.

(Fig. 1A, 2A, and B) demonstrates that *S100A4* alone is non-oncogenic, consistent with previous results in our *S100A4* transgenic mice (33). The increases in Ras and GFP proteins of 3.5- to 4-fold (Table 1) are consistent with the increase in GFP fluorescence of about 4-fold (Fig. 2B) and probably represent the increase in overall tumor mass between the Ras^{Val12} and the $Ras^{Val12}/S100A4$ larvae.

In agreement with different genetically manipulated *Ras* oncogenic systems in *Drosophila* (16, 18), the levels of endogenous activated phospho-JNK and MMP1 rise significantly in $Ras^{Val12}/S100A4$ compared with Ras^{Val12}larvae (Table 1). The rise in MMP1 protein is of the same order as the increase in fluorescently-labeled antibodies to MMP1. That JNK is indeed a downstream effector of $Ras^{Val12}/S100A4$ for metastasis is demonstrated by the reduction in the number with metastases and their ASSM in female Bsk^{DN}-expressing larvae compared to the male unsuppressed larvae (Fig. 2C). That these suppressed values for $Ras^{Val12}/S100A4$ are not significantly different from those of the Ras^{Val12} larvae (Fig. 2C) suggests that the predominant driver of the JNK–link to metastasis is the overexpression of S100A4. The 4.7-fold fall in the immuno-fluorescently-detectable β-galactosidase in the female, suppressed $Ras^{Val12}/S100A4$ larvae demonstrates that JNK needs to be activated to stimulate metastasis. Because of the level of JNK protein is relatively constant between Ras^{Val12} and $Ras^{Val12}/S100A4$ larvae (Table 1), S100A4 probably triggers activation of JNK by stimulating its increase in phosphorylation (24). Results using 10 μmol/L JNK-IN-8 confirm that JNK-induced phosphorylation of c-Jun is a necessary step in the S100A4–triggered pathway for metastasis. That there is a fall in CIFI for immunofluorescently detectable MMP1 (Fig. 3B) positions JNK before MMP in any pathway (16). Moreover, the fact that the MMP1 inhibitor, batimastat (25) inhibits ASSM and CIFI for GFP in the $Ras^{Val12}/S100A4$ larvae places MMP1 on the direct pathway to metastasis. The order of this novel S100A4-induced metastatic pathway is: S100A4→phospho-JNK→c-Jun→MMP1→metastasis. Thus, S100A4 appears to replicate the loss of function of suppressor genes *scrib* and *lethal2* (17) or *Her2* activation in the JNK/MMP pathway (16, 18). In transgenic mice or chemically transformed rat mammary cells, S100A4 combines with oncogenic *Neu* (*Her2*;

ref. 6) or *Ras* (4), respectively to stimulate, via the cytoskeleton, cell migration, and then subsequent events for invasion/metastasis (34). However, the involvement of this novel pathway has hitherto been unreported.

The relevance of our unique *Drosophila* model for S100A4 has been pursued in human breast cancer. IHC staining of our cohort of 183 breast carcinomas for the individual MMPs2, 9, 13 demonstrates 15% to 47% primary tumors are stained positively using a cut-off of 5%, in approximate agreement with previous reports (35, 36). Here we show that the overall duration of survival of patients with positively-stained carcinomas is highly significantly worse than for those patients classified as not staining for one of MMP2, 9, or 13 (Fig. 5), in agreement with results for MMP2 in hepatocarcinoma (37), skin melanoma (38) and for MMP13 in breast (36) and colon cancer (39). In contrast, MMP9 has been reported to be a favorable indicator in lymph-node-negative breast cancer (40). This favorable prognosis may depend on the much higher cutoff employed, because of our node-negative group showed no significant difference (Wilcoxon $\chi^2 = 2.63$, 1 df, $P = 0.11$). This difference was significantly greater for MMP9 staining in our node-positive patients ($\chi^2 = 18.40$, 1 df, $P < 0.001$). The other two MMPs showed similar significant differences in node-negative and node-positive patients (MMP2 $\chi^2 = 25.46$ and 25.39; MMP13 $\chi^2 = 14.91$ and 12.93, respectively). These results may suggest that MMP9 operates later than the other two MMPs at a post lymph-node-spreading stage in the disease process.

Overall, the RR of patient death in separate univariate analyses is greatest for patients with tumors stained for S100A4 (9.96), followed closely by those stained for MMP2 (9.04), then for MMP13 (4.87), and finally for MMP9 (4.69; Supplementary Table S3). However, the antibodies used here to detect the MMPs do not discriminate between inactive precursors or cleaved active MMPs and do not detect inhibitory TIMPs (41). Usually in cultured cells, S100A4 increases expression of MMP precursors and this results in an enhanced proteolytic activity and cell invasion/metastasis (42, 43). Moreover, S100A4 can act both intracellularly (43, 44) and extracellularly via RAGE receptors (45, 46) to stimulate MMP production. The fact that Bsk^{DN} inhibits S100A4-induced MMP1

and metastasis to the VNC in our *Drosophila* model (Fig. 2C and D) suggests that MMP1 is produced by the tumor cells and not by reactive stromal cells (47), consistent with immunohistochemical results in our human breast cancers. In contrast to the *Drosophila* model, the three JNK proteins in human cancers can exert both pro- and anti-oncogenic effects depending on the cell type and cross-talk with other kinases (48, 49). Thus, the oncogenic effect of activated JNK cannot be determined in human cancers from the measurement of its level alone, and hence was not attempted here.

Upon manipulation in cultured cells, S100A4 has been reported to control production of a single MMP, one of MMP2, 9, or 13, depending on the source and sometimes the report (42–45). In contrast, we show here that positive staining for each MMP2, 9, or 13 is separately and in combination very strongly associated with S100A4 and to a lesser extent with S100P (Table 2). The significant association of staining for MMP2, 9 with the basal cell markers CK5/6, CK14 has been reported previously (50), predominantly placing these MMPs, together with S100A4 and S100P, in the most aggressive subtype of breast cancers (26). When tested for RA of staining for S100A4 with the other three MMPs together, S100A4 is more likely to occur with MMP2, and the higher significant RA of MMP2 for S100A4 over a combination of other proteins confirms this result (Supplementary Table S6). Thus, S100A4 is more associated with MMP2, 13, and S100P more with MMP9, at least at the cellular level (Supplementary Table S6). This differential association in the tumor raises the novel possibility of synergistic interactions between the S100 proteins (29) occurring via different target MMPs.

Multiple longitudinal comparisons with survival time for all three MMPs together in multivariate analysis shows that only MMP2 and MMP9 are independently significant, whereas the contribution of MMP13 is confounded by that due to the other two MMPs (Supplementary Table S3). These results suggest partial overlap occurs between MMP2/MMP9-related pathways and MMP13-related pathways, whereas those related to MMP2 and MMP9 are more separate. This result is consistent with their function, MMP13 is a collagenase which is required to cut collagen fibrils first, before the two gelatinases, MMP2 or MMP9, can digest the remainder (51). When S100A4 and each MMP are tested in combination, the order of reduction in RR for S100A4 is MMP2 (42% reduction), then MMP13 (27% reduction) and finally MMP9 (11% reduction), whereas the reduction in RR for each MMP separately with S100A4 is similar (44%, 40%, and 43%,

respectively; Supplementary Table S3). These results suggest the pathways that S100A4 may trigger leading to premature death from metastatic disease overlap, to some extent, with those triggered by the three MMPs, the most overlap being with MMP2-related and then with MMP13-related pathways. The results for the close association of S100A4 and MMP2 are confirmed at the level of the cell where 91% of S100A4-containing cells also contain MMP2 and 96% of MMP2-containing cells also contain S100A4 (Supplementary Fig. S7). The considerable enhancing effect of S100P on S100A4-linked patient demise (29) may then be attributable, at least in part, to S100P targeting different MMPs from those targeted by S100A4 (Supplementary Table S6). This differential targeting of MMPs by S100 proteins is a novel mechanism for generation of the known synergy between different MIPs in the development of many cancers.

Disclosure of Potential Conflicts of Interest

Authors' Contributions

Conception and design: T.M. Ismail, D. Bennett, R. Barraclough, P.S. Rudland
Development of methodology: T.M. Ismail, D. Bennett, A.M. Platt-Higgins, P.S. Rudland
Acquisition of data (provided animals, acquired and managed patients, provided facilities, etc.): T.M. Ismail, D. Bennett, P.S. Rudland
Analysis and interpretation of data (e.g., statistical analysis, biostatistics, computational analysis): T.M. Ismail, D. Bennett, A.M. Platt-Higgins, M. Al-Medhity, P.S. Rudland
Writing, review, and/or revision of the manuscript: T.M. Ismail, D. Bennett, A.M. Platt-Higgins, M. Al-Medhity, R. Barraclough, P.S. Rudland
Administrative, technical, or material support (i.e., reporting or organizing data, constructing databases): T.M. Ismail, A.M. Platt-Higgins, P.S. Rudland
Study supervision: T.M. Ismail, P.S. Rudland

Grant Support

References

1. Dunnington DJ, Hughes C, Monaghan P, Rudland PS. Phenotypic instability of rat mammary tumor epithelial cells. J Natl Cancer Inst 1983;71: 1227–40.
2. Dunnington DJ, Kim U, Hughes CM, Monaghan P, Ormerod EJ, Rudland PS. Loss of myopepithelial cell characteristics in metastasizing rat mammary tumors relative to their nonmetastasizing counterparts. J Natl Cancer Inst 1984;72:455–66.
3. Steeg PS. Tumour metastasis: mechanistic insights and clinical challenges. Nat Med 2006;12:895–904.
4. Davies BR, Davies MP, Gibbs FE, Barraclough R, Rudland PS. Induction of the metastatic phenotype by transfection of a benign rat mammary epithelial cell line with the gene for p9ka, a rat calcium-binding protein, but not with the oncogene EJ-ras-1. Oncogene 1993;82:99–1008.
5. Barraclough R, Savin J, Dube SK, Rudland PS. Molecular cloning and sequence of the gene for p9Ka. A cultured myoepithelial cell protein with strong homology to S-100, a calcium-binding protein. J Mol Biol 1987;198:13–20.
6. Davies MP, Rudland PS, Robertson L, Parry EW, Jolicoeur P, Barraclough R, et al. Expression of the calcium-binding protein S100A4 (p9ka) in MMTV-neu transgenic mice induces metastasis of mammary tumours. Oncogene 1996;13:1631–7.
7. Rudland PS, Platt-Higgins A, Renshaw C, West CR, Winstanley JH, Robertson L, et al. Prognostic significance of the metastasis-inducing protein S100A4 (p9ka) in human breast cancer. Cancer Res 2000;60:1595–603.
8. Mazzucchelli L. Protein S100A4: too long overlooked by pathologists? Am J Pathol 2002;160:7–13.
9. Jenkinson SR, Barraclough R, West CR, Rudland PS. S100A4 regulates cell motility and invasion in an in vitro model for breast cancer metastasis. Br J Cancer 2004;90:253–62.
10. Gross SR, Sin CG, Barraclough R, Rudland PS. Joining S100 proteins and migration: for better or for worse, in sickness and in health. Cell Mol Life Sci 2014;71:1551–79.
11. Bazigou E, Apitz H, Johansson J, Loren CE, Hirst EM, Chen P-L, et al. Anterograde Jelly belly and Alk receptor tyrosine kinase signalling mediate retinal axon targeting in *Drosophila*. Cell 2007;128:961–75.
12. Halder G, Callaerts P, Flister S, Walldorf U, Kloter U, Gehring WJ. Eyeless initiates the expression of both sine oculis and eyes absent

during *Drosophila* compound eye development. Development 1998;125:2181–91.

13. Hauck B, Gehring W, Walldorf U. Functional analysis of an eye specific enhancer of the eyeless gene in *Drosophila*. Proc Natl Acad Sci U S A 1999;96:564–9.

14. Belvin MP, Anderson KV. A conserved signalling pathway: the *Drosophila* toll-dorsal pathway. Ann Rev Cell Biol 1996;12:393–416.

15. Bennett D, Lyulcheva E, Cobbe N. *Drosophila* as a potential model for ocular tumours. Ocul Oncol Pathol 2015;1:190–9.

16. Uhlirova M, Bohmann D. JNK- and FOS-regulated Mmp1 expression cooperates with Ras to induce invasive tumours in *Drosophila*. EMBO J 2006;25:5294–304.

17. Brumby AM, Richardson HE. Scribble mutants cooperate with oncogenic Ras or Notch to cause neoplastic overgrowth in *Drosophila*. EMBO J 2003;22:5769–79.

18. Duffy JB. GAL4 system in *Drosophila*. A fly geneticist's Swiss army knife. Genesis 2002;34:1–15.

19. Evans PC, Smith TS, Lai MJ, Williams MG, Burke DF, et al. A novel type of deubiquitinating enzyme. J Biol Chem 2003;278:23180–6.

20. Ismail TM, Fernig DG, Rudland PS, Terry CJ, Wang G, et al. The basic C-terminal amino acids of calcium-binding protein S100A4 promote metastasis. Carcinogenesis 2008;29:2259–66.

21. Ciurciu A, Duncalf L, Jonchere V, Lansdale N, Vasieva O, Glenday P, et al. PNuTs/PP1 regulates RNAPII-mediated gene expression and is necessary for developmental growth. PLOS Genetics 2013;9e1003885.

22. Baranski TJ, Cagan RLinventor; Washington University, assignee. Transgenic *Drosophila* and methods of use thereof. WO2009055461A1. 2009 Apr 30.

23. McCloy RA, Rogers S, Caldon CE, Lorca T, Castro A, Burgess A, et al. Partial inhibition of cdk1 in G2 phase overrides the SAC and decouples mitotic events. Cell Cycle 2014;13:1400–12.

24. Zhang T, Inesta-Vaquera F, Niepel M, Zhang J, Ficarro SB, Machleidt T, et al. Discovery of selective covalent inhibitions of JNK. Chem Biol 2012;19: 140–54.

25. Sledge GWJr, Qulai M, Goulet R, Bone EA, Fife R. Effect of matrix metalloproteinase inhibitor batimastat on breast cancer regrowth and metastasis in athymic mice. J Natl Cancer Inst 1995;87:1546–50.

26. de Silva Rudland S, Platt-Higgins A, Winstanley JHR, Jones NJ, Barraclough R, West CR, et al. Statistical association of basal cell keratins with metastasis-inducing proteins in a prognostically unfavorable group of sporadic breast cancers. Am J Pathol 2011;79:1061–72.

27. Rudland PS, Platt-Higgins A, Davies LM, de Silva Rudland S, Wilson JB, Aladwani A, et al. Significance of the Fanconi anemia FANCD2 protein in sporadic and metastatic human breast cancer. Am J Pathol 2010;176: 2935–47.

28. Orgaz JL, Pandya P, Dalmeida R, Karagiannis P, Sanchez-Loorden B. Diverse matrix metalloproteinase functions regulate cancer amoeboid migration. Nat Commun 2015;5:4255–70.

29. Wang G, Platt-Higgins A, Carrol J, de Silva Rudland S, Winstanley J, Barraclough R, et al. Induction of metastasis by S100P in a rat mammary model and its association with poor survival of breast cancer patients. Cancer Res 2006;66:1199–207.

30. Glasheen BM, Kabra AT, Page-McCaw A. Distinct functions for the catalytic and hemopexin domains of *Drosophila* matrix metalloproteinase. Proc Natl Acad Sci U S A 2009;106:2659–64.

31. Verma RP, Hansch C. Matrix metalloproteinases (MMPs): chemical-biological functions and (Q) SARs. Bioorg Med Chem 2007;15:2223–68.

32. Sorlie T, Tibshirani R, Parker J, Hastie T, Marron JS, Nobel A, et al. Repeated observation of breast tumor subtypes in independent gene expression data sets. Proc Natl Acad Sci U S A 2003;100:8418–23.

33. Davies M, Harris S, Rudland PS, Barraclough R. Expression of the rat, S-100-related, calcium-binding protein gene, p9Ka, in transgenic mice demon-strates different patterns of expression between these two species. DNA Cell Biol 1995;14:825–32.

34. Du M, Wang G, Ismail TM, Gross S, Fernig DG, Barraclough R, et al. S100P dissociates myosin IIA filaments and focal adhesion sites to reduce cell adhesion and enhance cell migration. J Biol Chem 2012;287: 15330–44.

35. Hao X, Sun B, Hu L, Lahdesmaki H, Dunmire V, Feng Y, et al. Differential gene and protein expression in primary breast malignancies and their lymph node metastases as revealed by combined cDNA microarray and tissue microarray analysis. Cancer 2004;100:1110–22.

36. Zhang B, Cao X, Liu Y, Cao W, Zhang F, Zhang S, et al. Tumour-derived matrix metalloproteinase-13 (MMP13) correlations with prognosis. BMC Cancer 2008;8:183–84.

37. Sze KM, Wong KL, Chu GK, Lee JM, Yau TO, Ng OP-L, et al. Loss of phosphatase and tensin homolog enhances cell invasion and migration through AKT/Sp-1 transcription factor/matrix metalloproteinase 2 activation in hepatocellular carcinoma and has clincopathologic significance. Hepatology 2011;53:1558–69.

38. Rotte A, Martinka M, Li G. MMP2 expression is a prognostic marker for primary melanoma patients. Cell Oncol 2012;35:207–16.

39. Yang B, Gao J, Rao Z, Shen Q. Clinicopathological significance and prognostic value of MMP-13 expression in colorectal cancer. Scand J Clin Lab Invest 2012;72:501–5.

40. Scorilas A, Karameris A, Arnogiannaki N, Ardavanis A, Bassilopoulous P, Trangas T, et al. Overexpression of matrix-metalloproteinase-9 in human breast cancer: a potential favourable indicator in node-negative patients. Br J Cancer 2001;84:1488–96.

41. Deryugina EI, Quingley JP. Matrix metalloproteinases and tumour metastasis. Cancer Metastasis Rev 2006;25:9–34.

42. Schmidt-Hansen B, Klingelhofer J, Grum-Schwensen B, Christensen A, Andresen S, Kruse C, et al. Functional significance of metastasis-inducing S100A4 (Mts1) in tumor-stroma interplay. J Biol Chem 2004;279:24498–504.

43. Zhang J, Zhang DL, Jiao XL, Dong Q. S100A4 regulates migration and invasion in hepatocellular carcinoma HepG2 cells via NF-κB-dependant MMP-9 signal. Eur Rev Med Pharmacol Sci 2013;17:2372–82.

44. Jia W, Gao XJ, Zhang ZD, Yang ZX, Zhang G. S100A4 silencing suppresses proliferation, angiogenesis and invasion of thyroid cancer cells through downregulation of MMP-9 and VEGF. Eur Rev Med Pharmacol Sci 2013;17:1495–508.

45. Yammani RR, Carlson CS, Bresnick AR, Loeser RF. Increase in production of matrix metalloproteinase 13 by human articular chondrocytes due to stimulation with S100A4: role of the receptor for advanced glycation end products. Arthritis Rheum 2006;54:2901–11.

46. Schmidt-Hansen B, Ornås D, Grigorian M, Klingelhöfer J, Tulchinsky E, Lukanidin E, et al. Extracellular S100A4(mts1) stimulates invasive growth of mouse endothelial cells and modulates MMP-13 matrix metalloproteinase activity. Oncogene 2004;23:5487–95.

47. Heppner KJ, Matrisian LM, Jensen RA, Rodgers WH. Expression of most metalloproteinase family members in breast cancer represents a tumor-induced host response. Am J Pathol 1996;149:273–82.

48. Wagner EF, Nebreda AR. Signal integration by JNK and p38 MAPK pathways in cancer development. Nat Rev Cancer 2009;9:537–49.

49. Cellurale C, Gimuis N, Jiang F, Cavanagh-Kyros J, Lu S, Garlick DS, et al. Role of JNK in mammary gland development and breast cancer. Cancer Res 2012;72:472–81.

50. Radenkovic S, Konjevic G, Jurisic V, Karadzic K, Nikitovic M, Gopcevic K, et al. Values of MMP-2 and MMP-9 in tumour tissue of basal-like breast cancer patients. Cell Biochem Biophys 2014;68:143–52.

51. Sela-Passwell N, Rosenblum G, Shoham T, Sagi I. Structural and functional bases for allosteric control of MMP activities: can it pave the path for selective inhibition? Biochim Biophys Acta 2010;1803:29–38.

Q11:   Page: 9: Author: Ref. 7 has been updated as per PubMed. Please verify.

Q12:   Page: 10: Author: Please verify Ref. 22 as typeset for correctness.

AU: Below is a summary of the name segmentation for the authors according to our records. The First Name and the Surname data will be provided to PubMed when the article is indexed for searching. Please check each name carefully and verify that the First Name and Surname are correct. If a name is not segmented correctly, please write the correct First Name and Surname on this page and return it with your proofs. If no changes are made to this list, we will assume that the names are segmented correctly, and the names will be indexed as is by PubMed and other indexing services.

First Name	Surname
Thamir M.	Ismail
Daimark	Bennett
Angela M.	Platt-Higgins
Morteta	Al-Medhity
Roger	Barraclough
Philip S.	Rudland